This article was downloaded by:[New York University]
[New York University]
On: 16 July 2007
Access Details: [subscription number 769426389]
Publisher: Taylor & Francis
Informa Ltd Registered in England and Wales Registered Number: 1072954
Registered office: Mortimer House, 37-41 Mortimer Street, London W1T 3JH, UK

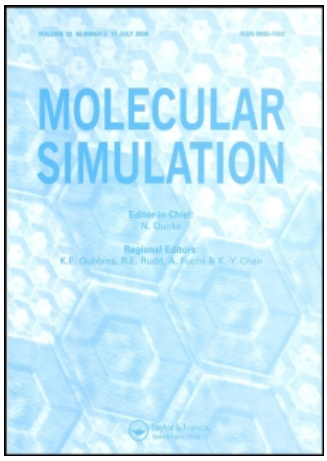

Molecular Simulation
Publication details, including instructions for authors and subscription information:
http://www.informaworld.com/smpp/title~content=t713644482

Evaluation of the Adaptive Umbrella Sampling Method

Mihaly Mezei [a]
[a] Department of Chemistry and Center for Study in Gene Structure and Function, Hunter College of the CUNY. New York, NY. USA

Online Publication Date: 01 August 1989
To cite this Article: Mezei, Mihaly , (1989) 'Evaluation of the Adaptive Umbrella Sampling Method', Molecular Simulation, 3:5, 301 - 313
To link to this article: DOI: 10.1080/08927028908031382
URL: http://dx.doi.org/10.1080/08927028908031382

PLEASE SCROLL DOWN FOR ARTICLE

Full terms and conditions of use: http://www.informaworld.com/terms-and-conditions-of-access.pdf

This article maybe used for research, teaching and private study purposes. Any substantial or systematic reproduction, re-distribution, re-selling, loan or sub-licensing, systematic supply or distribution in any form to anyone is expressly forbidden.

The publisher does not give any warranty express or implied or make any representation that the contents will be complete or accurate or up to date. The accuracy of any instructions, formulae and drug doses should be independently verified with primary sources. The publisher shall not be liable for any loss, actions, claims, proceedings, demand or costs or damages whatsoever or howsoever caused arising directly or indirectly in connection with or arising out of the use of this material.

© Taylor and Francis 2007

Molecular Simulation, 1989, Vol. 3, pp. 301–313
Reprints available directly from the publisher
Photocopying permitted by license only

© 1989 Gordon and Breach Science Publishers S.A.
Printed in Great Britain

EVALUATION OF THE ADAPTIVE UMBRELLA SAMPLING METHOD

MIHALY MEZEI

Department of Chemistry and Center for Study in Gene Structure and Function, Hunter College of the CUNY, New York, NY 10021, USA

(*Received December, 1988*)

The adaptive umbrella sampling technique, introduced recently to improve the probability ratio method and found to perform more reliably than the customary harmonic umbrella sampling, is tested and compared with other free energy methods. One of the tests applies the method to a transition involving a chemical change: calculation of the hydration free energy difference between acetone and dimethylamine and the other test calculates the conformational free energy difference between the C_7 and α_R conformations of the alanide dipeptide. The dipeptide problem is also treated by two types of thermodynamic integrations and by the perturbation method. The result for the acetone–dimethylamine problem is compared with previous calculations on the same system using the perturbation method, overlap ratio method and finite difference thermodynamic integration. Enhancements to the adaptive umbrella sampling method are also presented.

KEY WORDS: Free energy, Monte Carlo computer simulation, probability ratio method, adaptive umbrella sampling, alanine dipeptide.

1. INTRODUCTION

Methods for the calculation of free energy from computer simulations have been periodically reviewed in recent years [1–7]. Most methods fall into one of the following three classes: thermodynamic integration, the perturbation method and methods involving probability ratios. A comparison between the perturbation method and thermodynamic integration using three different paths has been described recently on the occasion of introducing a new variant of thermodynamic integration [8]; the methods were used to calculate the hydration free energy difference between dimethyl amine and acetone. In another set of calculations on the same problem the overlap ratio method was examined [13]. The purpose of this paper is to further study one of the methods involving probability ratios, the so called probability ratio method in conjunction with the adaptive umbrella sampling (*vide infra*), on both conformational and chemical transitions. The results will be compared with calculations using both thermodynamic integration and the perturbation method on the same system. Enhancements to the adaptive umbrella sampling method that have been developed during the course of these calculations will also be presented.

2. BACKGROUND

Calculations of the configurational free energy difference

$$\Delta A = A_1 - A_0 = -kT \ln (Z_1/Z_0), \tag{1}$$

from computer simulation on complex systems generally follow one of the three

techniques mentioned earlier, the thermodynamic integration (in the following, TI), originated from Kirkwood [10]:

$$\Delta A = \int_0^1 \delta A(\lambda)/\delta\lambda \, d\lambda = \tag{2a}$$

$$\int_0^1 \langle \delta E_N(\lambda)/\delta\lambda \rangle_\lambda \, d\lambda \tag{2b}$$

the perturbation method (in the followings: PM), proposed by Bennett [11] and Torrie and Valleau [12]:

$$\Delta A = -kT \ln \langle exp[-(E_1 - E_0)/kT] \rangle_0, \tag{3}$$

and methods involving probability ratios. These methods involve the acceptance ratio method of Bennett [11], the overlap ratio method developed by Jacucci and Quirke [9] (in the following, OR) and the probability ratio method (in the following, PRM) under consideration in this study. It was originally developed for the determination of the potential of mean force [14], and first applied to the determination of free energy differences by Mezei, Mehrotra and Beveridge [15]:

$$\Delta A = -kT \ln [P(\lambda)_{\lambda=1}/P(\lambda)_{\lambda=0}]. \tag{4}$$

In Equations (1–4) T is the absolute temperature, k is the Boltzmann factor, E_0 and E_1 are the energies of system 0 and 1, respectively, $E_N(\lambda)$ is the total configurational energy of an intermediate configuration with coupling parameter λ and $P(\lambda)$ is the Boltzmann probability of the system to be at the intermediate stage λ when λ is also a variable during the simulation. The coupling parameter λ describes a continuous path between the two systems as it varies from 0 to 1. In general several such paths exist (three different ones were examined in Reference [8] for the acetone–dimethyl amine problem). Most of the calculations described in this paper follow a path that transforms linearly the coordinates of the molecule(s) changed, along with the potential coefficients (whenever applicable), resulting in a continuous deformation of system A into system B along a non-linear path (the dependence of $E(\lambda)$ is not linear in λ). For this path, at each λ the coordinates of the "hybrid molecule" are obtained as

$$R(\lambda) = (1 - \lambda) R^A + \lambda R^B, \tag{5}$$

Where R_A and R_B are the coordinates of the original molecules A and B, respectively. When the systems A and B differ chemically as well, similar coupling is performed on the solute-solvent potential coefficients (e.g. the R vectors include the potential coefficients).

For the dipeptide problem thermodynamic integration was also performed over the path

$$E(\lambda, X^N) = \lambda^k E_1(X^N) + (1 - \lambda)^k E_0(X^N). \tag{6}$$

proposed by Mezei and Beveridge [6] and tested by Mezei [8, 16, 17]. In this case system A is continuously turned off while system B is turned on. The exponent k was introduced to eliminate the singularity first treated by Mruzik *et al.* [18].

The potential of mean force along λ is defined as:

$$W(\lambda) = -kT \ln P(\lambda) + \text{const.} \tag{7}$$

For free energy changes above a few kT, Equation (7) implies that the probabilities of sampling of the two conformations would differ by orders of magnitude. Thus,

when the coupling parameter λ is also a simulation variable, in order to take advantage of Equation (7), the simulation has to be performed in a non-Boltzmann ensemble, where the Hamiltonian $E(X^N, R(\lambda))$ is replaced by a modified Hamiltonian $E'(X^N, R(\lambda))$:

$$E'(X^N, R(\lambda)) = E(X^N, R(\lambda)) + E_w(\lambda). \tag{8}$$

The Boltzmann average of any quantity Q can be recovered as

$$\langle Q \rangle_B = \langle Q w(\lambda) \rangle_w / \langle w(\lambda) \rangle_w \tag{9}$$

where

$$w(\lambda) = exp\,[E_w(\lambda)/kT] \tag{10}$$

and $\langle\,\rangle_w$ implies configurational average using the modified Hamiltonian given by Equation (8). Use of this technique is usually referred to as umbrella sampling. Most previous calculations using umbrella sampling used an empirical approach to determine the non-Boltzmann bias. In particular, Pangali, Rao and Berne introduced the harmonic weighting function [19]:

$$E_w(\lambda) = c(\lambda - \lambda_0)^2 \tag{11}$$

where the simulation is designed to sample in the vicinity of λ_0.

Recently, iterative approaches have been developed, based on the recognition of the fact that the best choice for $E_w(\lambda)$ is $-W(\lambda)$. Paine and Scheraga [20] obtained the gas-phase conformational free energy map of the alanine dipeptide and Mezei [21] recalculated the free energy difference between the C_7 and α_R conformations of the alanine dipeptide in aqueous solution. For the latter problem, several technical difficulties had to be overcome: matching of iterations with large statistical noise, recognition of equilibration phase, guiding the simulation to undersampled regions and others. An important element of the method is the recognition that the normalization factors of the estimated probability distributions (whose determination is equivalent of the "matching" problem discussed in previous studies) should be continually redetermined as the calculation proceeds through the solution of a nonlinear minimization problem. Using this iterative scheme is called adaptive umbrella sampling (in the followings: AUS). In recent work on the calculation of the conformational free energy of the dimethyl phosphate anion the AUS method proved to be significantly more reliable than the use of the harmonic weighting function [22].

The first test, transforming acetone into dimethylamine in dilute aqueous solution, allows for detailed comparison with several earlier calculations and gives the first indication as to the performance of the AUS–PRM method on a chemical transition.

The second test system treats only conformational transformation, the change from C_7 to α_R conformation of the alanine dipeptide, but it involves a larger change and thus provides information on the scaling properties of the methods compared. Previous studies [15, 21] (using the potential library of Clementi and coworkers [23]) have shown that the solvent effect prefers the α_R conformation. Thus, the current study, besides providing information on the performance of the AUS—PRM method, will show the sensitivity of the calculated free energy difference to the choice of potentials. Comparisons with thermodynamic integrations along both paths described by Equations (5, 6) and with perturbation method calculations will be also given.

Table 1 Results of the PRM method calculations for the acetone-dimethylamine problem

λ_-	λ_+	*Half-time results*				*Final results*					
		PRM1	*PRM2*	*PRM4*	*PRM5*	*PRM1*	*PRM2*	*PRM3*	*PRM4*	*PRM5*	*PRM5*
0.0	0.1	1.32	1.53	1.92	1.83	1.49	1.69		1.61	1.71	1.96
0.1	0.3	1.68	2.32	2.22	1.51	1.74	1.63		2.38	1.75	1.84
0.3	0.6	1.70	1.24	1.30	1.71	1.43	1.36		0.89	1.52	1.37
0.6	0.9	−0.82	−1.86	0.09	−0.91	−1.06	−1.03		−0.26	−0.81	−0.68
0.9	1.0	2.80	−3.06	2.11	−2.02	−2.52	−3.09	2.16	−2.45	−2.25	−2.13
0.0	0.9	3.75	3.88	5.47	4.25	3.60	3.65		4.62	4.16	4.49
0.0	1.0	1.06	0.17	3.36	2.23	1.07	0.55	1.44	2.17	1.91	2.36
	MC steps:	2000 K	2000 K	2000 K	2000 K	3800 K	4000 K	1000 K	3800 K	4000 K	6000 K

λ_-, λ_+ are the end point coupling parameter values: All energies are in kcal/mol: $\lambda = 0$. (acetone) $\lambda = 1$. (dimethylamine); PRM1 and PRM2 refer to the probability ratio method calculations with 50 K and 100 K iterations, respectively, PRM 3 refers to the calculation restricted to [0.85,1.0] interval and PRM4 and PRM5 refer to the probability ratio method calculations using 100 K long iterations with generating new starting point for the minimization at every 2nd and 5th iteration, respectively.

Table 2 Comparison of the free energy differences computed over intervals of the coupling parameter with TI, PM, OR and PRM.

λ_-	λ_+	*Half-time results*				*Final results*				
		PM	*TI*	*OR*	*PRM5*	*PM*	*TI*	*OR*	*PRM5*	*PRM5*
0.0	0.1	1.45	1.33		1.83	1.34	1.35		1.71	1.96
0.1	0.3	2.09	2.19		1.51	2.09	2.20		1.75	1.84
0.0	0.3	3.54	3.52	3.73	3.34	3.43	3.55	3.70	3.46	3.80
0.3	0.6	1.28	1.30		1.71	1.26	1.33		1.52	1.37
0.6	0.9	−0.89	−1.09		−0.91	0.88	1.13		−0.81	−0.68
0.9	1.0	−1.67	1.61	−1.72	−2.02	−1.70	−1.58	1.76	−2.25	−2.13
0.0	1.0	2.25	2.14	2.56	2.23	2.11	2.17	2.27	1.91	2.36
	Run length:	4500 K	4500 K	2000 K	2000 K	7000 K	7000 K	3800 K	4000 K	6000 K

λ_-, λ_+ are the end point coupling parameter values: The TI result for the interval was obtained by integrating the polynomial of the Gaussian quadrature: All energies are in kcal/mol: $\lambda = 0$ (acetone), $\lambda = 1$ (dimethylamine); PRM5 refers to the probability ratio method calculations using 100 K iterations with generating new starting point for the minimization at every 5th iteration.

3. CALCULATIONS

The simulations used the Metropolis algorithm [24], modified by incorporating the force bias procedure [25] and preferential sampling [26] for convergence acceleration. The energy calculations were based on the OPLS functions developed by Jorgensen and coworkers for the solute-water interactions [27, 28] and the TIP4P water-water potential [29, 30]. These parameters were developed to represent the interactions between water and small amides; however, for lack of more specific parameters they were also used for acetone and dimethyl amine. Clearly, this is an extrapolation and thus for the acetone-dimethylamine problem the comparison with experimental data could be expected to be worse than usual with the OPLS potentials.

The alanine dipeptide, AcAlaNHMe, is customarily described by the torsion angles ψ (N–C–C–N) and ϕ (C–N–C–C). The conformation preferred in the gas phase called C_7 corresponds to torsion angles $\psi = 90°$, $\phi = -90°$ and the conformation modeling the α-helix, called α_R is described here with torsion angles $\psi = -50°$ and $\phi = -70°$.

The essence of the PRM is that the coupling parameter λ (defined for this study by Equation (5)) is also varied during the simulation. This work employed the adaptive umbrella method described in Reference [21]. In addition to the concerns raised in Reference [21], for the chemical transition care had to be taken to make sure that the coupling parameter never leaves the [0,1] interval. This is a consequence of the introduction of the coupling to the repulsive core term, whose sign could change upon the coupling parameter leaving the [0,1] interval, resulting in solvents being drawn onto the solute. This problem does not arise in PRM calculations where only conformational changes are considered.

The calculations described here used either 50 K iterations or 100 K iterations (1 K = 1000 attempted moves). The sampling of the whole interval was speeded up by using the extension scheme of Equation (19) of Reference 21 with C = 0 and the newer extension scheme described in Appendix II with $c_m = 1.1$ and $c_r = 0.75$. The estimate of the probability distribution was improved by the technique described in Equation (21) of Reference [21] with $DW_{max} = 5kT$ and the technique described in Appendix III. The iteration screening procedure described in Appendix I was also employed, but it screened out only one iteration. However, on trial runs with $C = 0.2kT$ ("strong encouragement") it was very efficient to screen out the obviously unequilibrated iterations that resulted from the application of the too small C value. Calculations were also performed where the input to the minimization procedure (the initial values of the normalization factors) were periodically recomputed (as opposed to using the values from the previous iteration), as described in Appendix IV.

4. RESULTS AND DISCUSSION

Tables 1 and 2 summarize the computed free energy differences for the first test system (done without the regeneration of initial normalization factors) at the middle and at the end of the calculation using the PM and the TI along the same coupling parameter path from Reference [8], some of the OR calculations from Reference [13] and with the PRM used here, along with the run lengths involved. The comparison is extended to the free energy differences computed between intermediate states.

The 2000 K long PRM runs (labeled PRM1 and PRM2) already succeeded in sampling the full [0,1] interval and, except for the [0.9,1.0] interval where the "crea-

tion" of the oxygen atom has just started, gave results that are close to the TI, PM and OR values, at less than one third of the cost. In the [0.9,1.0] interval, however, the agreement was poor, due mainly to the general difficulty of simulating a creation regime and also to the finite coupling parameter gridsize (0.02) combined with the large gradient of $W(\lambda)$. Extending the calculation to 4000 K brought the cost close to the TI, PM or OR costs since the fitting procedure becomes rather expensive as the number of iterations reach the one hundred range but the precision did not improve significantly in this range.

The poor performance of the calculations on the creation region prompted an additional calculation where the coupling parameter was limited to the [0.85,1.0] range (labeled PRM3). 50 K iterations were used. Due to the restriction on λ, most iterations sampled the whole [0.9, 1.0] interval. As seen in Table 2, the agreement with the previous results improved significantly but some discrepancy still remained. It can be probably attributed to the fact that the calculation used a 0.02 gridsize to collect the coupling parameter distribution and the steep drop at the $\lambda = 0$ end (cca 1 kcal/mol difference between the gridpoints centered at 0.97 and 0.99) makes the results sensitive to the choice of grids and less certain the extrapolation from 0.99 to 1.0. This could only be improved by the use of a finer grid.

Since the PRM3 run showed that the method is capable to give results close to the TI, PM and OR results, it was thought that the possibility of the nonlinear minimization reaching a local minimum that is too far from the global minimum may be a factor in the poorer performance of the PRM1 and PRM2 runs on the [0.9,1.0] coupling parameter interval. To test this hypothesis, the normalization factors were recalculated for the run PRM2 with the procedure described in Appendix IV. This produced a $W(\lambda)$ that was virtually identical with the previously obtained one over the [0.0,0.9] interval but on the critical [0.9,1.0] interval the calculated free energy difference changed by 0.3 kcal/mol (in the right direction). This prompted two new calculations (labeled by PRM4 and PRM5) where the minimization started from a fresh initial estimate at every 2nd or 5th iteration, respectively. 100 K iterations were used to allow long runs without having to solve the minimization problem with too many iterations even though the 50 K iteration run performed better on the critical interval. Each calculation gives the free energy difference within a few tenth of a kcal/mol to the results with the other methods. The behaviour on the [0.9,1.0] coupling parameter interval is about as good as that of the PRM3 run. The comparisons on the subintervals, however still show larger deviations from the other runs and the change as the calculation progresses is larger than the corresponding change in either of the other runs over comparable length of the calculation indicating slower convergence. The calculation regenerating the starting point at every other iteration appears to perform somewhat worse than the one that regenerates the starting point only at every 5th iteration.

For the alanine dipeptide, the AUS–PRM calculation was performed in two steps, the first step sampled the coupling parameter interval [0,0.55] while the second was restricted on the [0.45,1.0] interval. As an additional test, a calculation was also done on the [0.35,0.65] interval. These calculations used 50 K iterations and their length was between 3200 and 3600 K. The calculated potential of mean force is shown in Figure 1. The solvent contribution to the free energy difference between the two conformation is obtained as 12.5 kcal/mol, favoring α_R, based on the three calculations (matched at the center of the overlapping segments) and as 12.8 kcal/mol using only the first

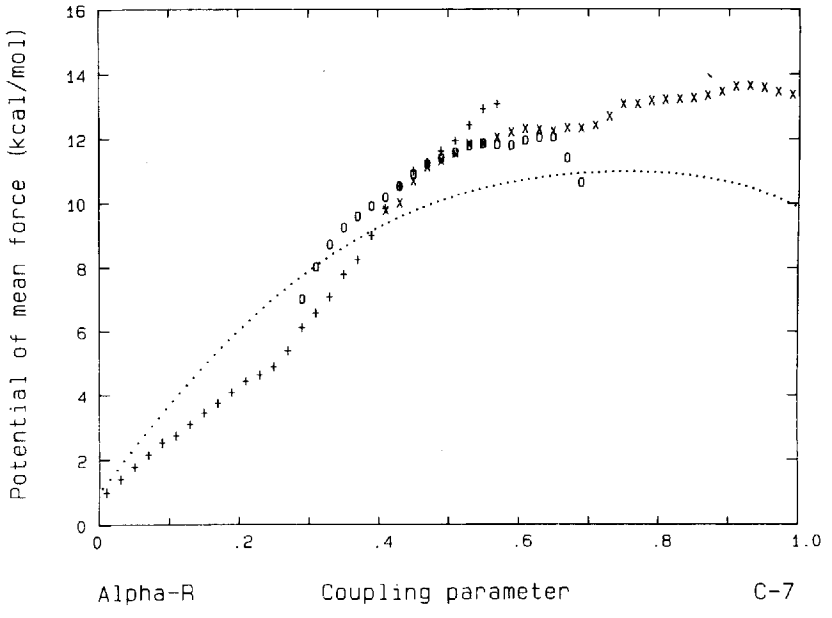

Figure 1 Potential of mean force for the C_7-α_R transformation of the alanine dipeptide. ..... : FDTI; ++++: PRM on the [0.0,0.55] interval; oooo: PRM on the [0.35,0.65] interval; xxxx: PRM on the [0.45,1.0] interval.

two runs. Based on the comparison of the potential of mean force estimates over the same λ interval, the uncertainty of these can be put at 1–2 kcal/mol. The direction of the difference is in agreement with both previous calculations [15, 21] and experimental estimates. Its magnitude, however, is significantly larger. Reference [15] calculated 3.6 kcal/mol that was revised in Reference [21] to 1.8 kcal/mol. The previous calculations used the potentials of Clementi and coworkers that assigned different charge parameters to different conformations. It is suspected that the large free energy difference is mainly due to the conformation independent charges used by the OPLS potentials. This issue is currently under investigation.

The adequate assessment of the performance of the AUS–PRM method required calculations on the same problem using different methods. Thus we calculated the free energy difference by thermodynamic integration over the path used by the PRM calculations described by Equation (5) and over the "nearly linear" path described by Equation (6). The integrand of Equation (2a) as approximated by a finite difference ratio of ΔA and $\Delta\lambda$ where $\Delta\lambda$ was chosen to be 0.02 and ΔA was computed by the PM. This technique, called finite difference thermodynamic integration, (FDTI) was suggested in Reference [8]. The potential of mean force calculated from TI is also shown on Figure 1. In addition, Table 3 gives the free energy differences at the quadrature points and the corresponding calculated conformational free energy differences calculated as the calculation progressed while Table 4 gives the TI integrands and calculated free-energy differences in a similar fashion.

The FDTI calculation, based on a 5-point Gaussian quadrature, gave the free energy difference as 8.9 ± 4.6 kcal/mol while the nearly linear TI gave

Table 3 Description of the FDTI calculations.

λ:	*5-point quad.*					*3-point quad.*			
	0.0469	*0.2308*	*0.5*	*0.7692*	*0.9531*	ΔA	*0.1127*	*0.8873*	ΔA
1000 K	0.5742	0.4009	0.1702	−0.0759	−0.1513	8.8	0.5152	−0.0044	10.8
2000 K	0.5350	0.4038	0.1455	−0.0627	−0.1350	8.6	0.5231	−0.1060	9.0
3000 K	0.5425	0.4014	0.1392	−0.0101	−0.1443	9.0		−0.0674	9.3
4000 K	0.5419	0.4026	0.1530	0.0135	−0.1512	9.5			
5000 K	0.5420	0.3932	0.1408	−0.0078	−0.1609	8.9			

The ΔA values are the calculated free energy differences. The other table entries are the free energy differences over the 0.02 wide λ intervals centered at the quadrature point; all energies are in kcal/mol

Table 4 Description of the nearly linear TI calculations.

λ:	*0.0469*	*0.2308*	*0.5*	*0.7692*	*0.9531*	ΔA
1000 K	204.38	62.839	3.5468	−54.599	−126.29	11.7
2000 K	209.69	61.163	1.8278	−47.434	−136.09	12.6
3000 K	205.34	63.948	0.7734	−46.662	−135.87	12.6
4000 K	200.02	62.532	0.9297	−48.057	−134.15	12.6

The ΔA values are the calculated free energy differences. The other table entries are the TI integrands at the quadrature points; all energies are in kcal/mol.

12.6 ± 3.0 kcal/mol. A somewhat shorter FDTI calculation using a 3-point quadrature gave 9.37 kcal/mol. The error estimates were obtained from the error estimates for the integrand at each quadrature point, calculated based on block averages. From the stability of the calculated free energy differences these estimates appear to be somewhat conservative although not out of line from the usual precision obtained on solute-solvent properties for such a solute size. The larger discrepancy between the FDTI and the other two results is likely due to interpolation error since the potential of mean force as calculated by the PRM appears to have a more complex shape.

Finally, two additional simulations attempted the calculation of the free energy difference over the [0.0,0.1] and [0.0, 0.15] intervals using the PM, to estimate the number of PM runs that would be needed to calculate the free energy difference adequately. The simulations used a Hamiltonian that corresponded to a state that is the average of the two endpoints, as described in Reference [8]. After 1500 K MC steps the free energy difference settled at 1.9 and 2.0 kcal/mol, respectively. These numbers are quite inconsistent with the estimate obtained from the PM calculations over the 0.02 λ intervals at $\lambda = 0.046$ and $\lambda = 0.11$, as both of them gave over 0.52 kcal/mol, suggesting 2.6 kcal/mol for just the [0.0,0.1] interval. A closer inspection of the PM calculations showed that the smallest and largest energy differences sampled spread over 14.8 and 19.2 kcal/mol, respectively, indicating that the smallest and largest terms contributing to Equation (3) would differ by factors of $\exp(14.8/kT) = 5.2 \times 10^{10}$ and $\exp(19.2/kT) = 7.9 \times 10^{13}$, respectively!

The calculations reported here present the probability ratio method with adaptive umbrella sampling as a competitive alternative to the OR, PM or TI for the calculation of solvation free energy differences involving small chemical change, although its slower convergence results in somewhat lower precision at comparable cost. However, the self-checking nature of the method ensures that the error is never too large since a significantly incorrect estimate for $W(\lambda)$ will lead to inadequate sampling of the coupling parameter space. It is also an advantage that the need to set up several individual calculations is absent (or, for more complex problems, largely reduced).

For the larger change examined in this study, the PRM and the nearly linear TI showed equally good performances; the other TI technique, FDTI, appeared to show some quadrature error and the PM was found to require too many steps and thus was deemed uneconomical.

Acknowledgements

This work was supported under an RCMI grant #SRC5G12RR0307 from NIH to Hunter College and a CUNY/PSC grant. Computing resources were provided by the City University of New York, University Computing Center. Stimulating discussion with Dr. R. Friedman are gratefully acknowledged.

APPENDIX I. A-POSTERIORI REJECTION OF ADAPTIVE UMBRELLA SAMPLING ITERATIONS

In Reference [21] it was suggested that upon reaching a new coupling parameter region the corresponding iteration(s) be dropped since these are likely to correspond to an "unequilibrated" state. It was also remarked that this procedure needs improvement since it is not clear a-priori, just how many iterations really need to be dropped.

This appendix describes a more sophisticated procedure that has been applied in the present work. At the end of every iteration, all iterations are compared with the subsequent ones. Those that are found to be followed by iterations sampling the same region but giving significantly different distribution are dropped. The term "significantly different" is given quantitative meaning as follows. For two iterations i and j the range of overlap [p,q] is determined first (p and q are the limiting gridpoints corresponding to the coupling parameter region sampled by both iterations). Iterations that are only marginally overlapping, that is, when $q - p \leqslant N^0_{min}$, are not compared. N^0_{min} was chosen to be 4, corresponding to a coupling parameter interval of length 0.08 in the simulation. For gridpoints $p \leqslant s \leqslant q$ the ratio

$$r_s = p^i_s/p^j_s \tag{A1.1}$$

and the weight

$$w_s = (N^i_s/N^j_s + N^j_s/N^i_s)(N^i_s + N^j_s) \tag{A1.2}$$

were computed where p^i_s is the probability distribution value at gridpoint s in iteration i and N^i_s is the number of times the gridpoint s was sampled in iteration i. The deviation index I_D was obtained as

$$I_D = \{[(\Sigma_s w_s r_s/\Sigma_s w_s)^2 - (\Sigma_s w_s r_s^2/\Sigma_s w_s)]/(q - p)\}^{1/2}. \tag{A1.3}$$

Clearly, for distributions that are identical, I_D is zero and larger deviations will give larger I_D values. The fundamental assumption in this screening procedure is that later interactions are less likely to be unequilibrated. On this basis the following rejection criterion was established: Drop any iteration that gives $I_D > I_D^{min}$ values with more than PC^{min} percent of the subsequent iterations. After some experimentation, the values $I_D^{min} = 0.9$ and $PC^{min} = 20\%$ was chosen.

APPENDIX II. A NEW SCHEME TO GUIDE THE SIMULATION TOWARD UNSAMPLED REGIONS

In the procedure described in Reference [21], the "abandonment" of a coupling parameter region triggered the introduction of a modification of the umbrella sampling weights designed to drive back the simulation whenever the overall sampling rate of the abandoned region was below a threshold value. The modification was always by a constant factor, given on input. This inflexibility reduced the efficiency of the procedure since too small change was ineffective while too large values resulted in clearly unequilibrated iterations. While the screening procedure described in Appendix I was rather successfull in removing these unequilibrated iterations during trial runs, it resulted in the deletion of too many iterations. In the present work a more flexible alternative has been employed as follows.

An array of additional biasing factors $S(\lambda_g)$ is established and initialized to 1. At the end of each iteration, the array elements corresponding to unsampled gridpoints are multiplied by a constant c_m (> 1) and for sampled gridpoints raised to the power of c_r (< 1), an other constant. The biasing weights computed from the E_w values just calculated are then multiplied by S. This way, unsampled grids become progressively more attractive while sampling of a grid will eliminate this added "attraction" in a few iterations. The ratio of the smallest and largest values in S also gives an indication of accuracy of the computed probability distribution — the larger this ratio, the stronger distortion of the computed E_w was required to obtain full sampling.

APPENDIX III. ELIMINATION OF SPURIOUS PEAKS FROM $w(\lambda)$

In Reference [21] it was suggested that the ratio of $w(\lambda)$ values (**e.g.** difference between $E_w(\lambda)$ values) corresponding to neighbouring grids be limited to a threshold value to screen out spurious jumps in $E_w(\lambda)$. In the present work an additional filter of the same vein has been introduced as follows.

For three consecutive gridpoints λ_{i-1}, λ_i, λ_{i+1}, the value of $w(\lambda_i)$ will be modified whenever it is outside of the interval

$$[0.75\ w(\lambda_{i-1}) + 0.25\ w(\lambda_{i+1}),\ 0.25\ w(\lambda_{i-1}) + 0.75\ w(\lambda_{i-1})], \tag{A3.1}$$

the "middle half" of the interval $[w(\lambda_{i-1}), w(\lambda_{i+1})]$. That is, if

$$|w(\lambda_i) - w(\lambda_{i-1})| < |w(\lambda_{i+1}) - w(\lambda_{i-1})|/4 \tag{A3.2}$$

then $w(\lambda_i)$ is replaced by

$$w(\lambda_{i-1}) + [w(\lambda_{i+1}) - w(\lambda_{i-1})]/4 \tag{A3.3}$$

and if

$$|w(\lambda_i) - w(\lambda_{i+1})| < |w(\lambda_{i+1}) - w(\lambda_{i-1})|/4 \tag{A3.4}$$

then $w(\lambda_i)$ is replaced by

$$w(\lambda_{i+1}) + [w(\lambda_{i+1}) - w(\lambda_{i-1})]/4. \tag{A3.5}$$

The underlying assumption in this procedure is that the grid is fine enough so that $w(\lambda_i)$ is a rather smooth function. This assumption is also important when a "legitimate" peak is encountered, since in that case the elimination of the peak introduces a small error. Actually, if this assumption is not fulfilled then the calculated $w(\lambda)$ would be sensitive to the gridsize and the position of the grid.

APPENDIX IV. GENERATING NEW STARTING VALUES FOR THE MINIMIZATION PROBLEM

The alternative to using the normalization coefficients from the previous iterations as a starting point for the minimization is based on the assumption that for iterations that cover the same coupling parameter range the normalization factors can be determined to a good approximation by the one-step optimization procedure described in Reference 21 where only the last iteration's normalization factor is allowed

to vary. The new approach starts with defining a center for each iteration i as

$$\lambda_{c,i} = \sum_k n(\lambda_k)\,\lambda_k / \sum_k n(\lambda_k) \qquad \text{(A4.1)}$$

where $n(\lambda_k)$ is the number of configurations with coupling parameter value falling into the grid centered at λ_k. The iterations are sorted in the order of increasing $\lambda_{c,i}$, the first iteration is assigned normalization factor 1. After that, the normalization factor of each successive iteration is determined by the one-step optimization process.

References

[1] J.A. Barker and D. Henderson, "What is 'Liquid'? Understanding the States of Matter," *Rev. Mod. Phys.*, **48,** 587 (1976).

[2] N. Quirke, "The Calculation of Free Energies Using Computer Simulation," *Proceedings of the NATO Summer School on Superionic Conductors,* Odense, Denmark, Plenum Press (1980).

[3] K.S. Shing and K.E. Gubbins, Advances in Chemistry Series, 204, Molecular Based Study of Fluids, J.M. Haile and G.A. Mansoori, eds., ACS, Washington (1983).

[4] Levesque, J.J. Weiss and J.P. Hansen, "Recent Developments in the Simulation of Classical Fluids," in *Monte Carlo Methods in Statistical Physics II,* K. Binder, ed., Springer Verlag, Berlin (1984).

[5] A. Pohorille and L.R. Pratt, Theoretical Methods for Obtaining Free Energies of Biomolecular Equilibria in Aqueous Solution," in *Methods in Enzymology, Biomembranes,* **127,** (1986).

[6] M. Mezei and D.L. Beveridge, "Free Energy Simulations," *Ann. Acad. Sci. N.Y.*, **482,** 1 (1986).

[7] D. Frenkel, in Molecular-Dynamics Simulation on Statistical Mechanical Systems, Soc. Italiana di Fisica, Bologna, 1986.

[8] M. Mezei, "The Finite Difference Thermodynamic Integration, Tested on Calculating the Hydration Free Energy Difference between Acetone and Dimethylamine in Water," *J. Chem. Phys.*, **86,** 7084 (1987).

[9] G. Jacucci and N. Quirke, *Molec Phys.*, **40,** 1005 (1980).

[10] J.G. Kirkwood, in "Theory of Liquids", B.J. Alder, ed., Gordon and Breach, New York (1968).

[11] C.H. Bennet, "Efficient Estimation of Free Energy Differences from Monte Carlo Data," *J. Comp. Phys.*, **22,** 245 (1976).

[12] G.M. Torrie and J.P. Valleau, "Nonphysical Sampling Distributions in Monte Carlo Free-Energy Estimation: Umbrella Sampling," *J. Comp. Phys.*, **23,** 187 (1977).

[13] M. Mezei, "Test of the Overlap Ratio Method on the Calculation of the Aqueous Hydration Free Energy Difference Between Acetone and Dimethyl Amine," *Molec. Phys.*, **64,** (1988).

[14] G. Patey and J.P. Valleau, *J. Chem. Phys.*, **63,** 2334 (1975).

[15] M. Mezei, P.K. Mehrotra and D.L. Beveridge, "Monte Carlo Determination of the Free Energy and Internal Energy of Hydration for the Ala Dipeptide," *J. Am. Chem. Soc.*, **107,** 2239 (1985).

[16] M. Mezei, "Direct Calculation of Excess Free Energy of the Dense Lennard-Jones Fluid with Nonlinear Thermodynamic Integration," *Molecular Simulation,* in press (1988).

[17] M. Mezei, in preparation.

[18] M.R. Mruzik, F.F. Abraham, D.E. Schreiber and G.M. Pound, "A Monte Carlo Study of Ion-Water Clusters," *J. Chem. Phys.*, **64,** 481 (1876).

[19] C.S. Pangali, M. Rao and B.J. Berne, "Potential of Mean Force for the Interaction of Noble Gas Atoms in Water," *J. Chem. Phys.*, **71,** 2975 (1979).

[20] G.M. Paine and H.A. Scheraga, "Prediction of the Native Conformation of a Polypeptide by a Statistical-Mechanical Procedure. I. Backbone Structure of Enkephalin," *Biopolymers,* **24,** 1391 (1985).

[21] M. Mezei, "Adaptive Umbrella Sampling: Self-Consistent Determination of the Non-Boltzmann Bias," *J. Comp. Phys.*, **68,** 237 (1987).

[22] B. Jayaram, M. Mezei and D.L. Beveridge, "Conformational Stability of Dimethylphosphate Anion in Water: Liquid State Free Energy Simulations," *J. Am. Chem. Soc.*, **110,** 1691 (1987).

[23] G. Corongiu and E. Clementi, "Intramolecular and Intermolecular Interactions for Deriving Chemical Formulae and for Simulate Complex Chemical Systems," *Gazz. Chim. Ital.*, **108,** 273 (1978).

[24] N.A. Metropolis, A.W. Rosenbluth, M.N. Rosenbluth, A.H. Teller and E. Teller, "Equation of State Calculation by Fast Computing Machines," *J. Chem. Phys.*, **21,** 1087 (1953).

[25] M. Rao, C.S. Pangali and B.J. Berne, "On the Force Bias Monte Carlo Simulation of Water: Methodology, Optimization and Comparison with Molecular Dynamics," *Mol. Phys.*, **37,** 1779 (1979).

[26] J.C. Owicki and H.A. Scheraga, "Preferential Sampling Near Solutes in Monte Carlo Calculations on Dilute Solutions," *Chem. Phys. Letts.*, **47,** 600 (1979); J.C. Owicki, "Optimization of Sampling Algorithms in Monte Carlo Calculations of Fluids," in *Computer Modeling of Matter,* P.G. Lykos, ed., (American Chemical Society, Washington, D.C., 1978).

[27] W.L. Jorgensen and C.J. Swenson, "Optimized Intermolecular Functions for Amides and Peptides. Structure and Properties of Liquid Amides," *J. Am. Chem. Soc.,* **107,** 569 (1985).

[28] W.L. Jorgensen and C.J. Swenson, "Optimized Intermolecular Functions for Amides and Peptides. Hydration of Amides," *J. Am. Chem. Soc.,* **107,** 1489 (1985).

[29] W.L. Jorgensen, J. Chandrashekar, J.D. Madura, R. Impey and M.L. Klein, "Comparison of Simple Potential Functions for Simulating Liquid Water," *J. Chem. Phys.,* **79,** 926 (1983).

[30] W.L. Jorgensen and J.D. Madura, "Temperature and Size Dependence for Monte Carlo Simulations of TIP4P Water," *Mol. Phys.,* **56,** 1381 (1985).